



1 Integrated Impact of Digital Elevation Model and Land Cover 2 Resolutions on Simulated Runoff by SWAT Model

3 Mahmoud Saleh Al-Khafaji¹, Fouad Hussein Al-Sweiti²

4 ¹Building and Construction Engineering Department, University of Technology, Baghdad, Iraq

5 ²Ministry of Water Resources, Baghdad, Iraq

6 *Correspondence to:* Mahmoud Saleh Al-Khafaji (41100@uotechnology.edu.iq)

7 **Abstract.** Complementary interactive effects of the Digital Elevation Model (DEM) and Land Cover (LC) resolutions on the
8 estimated runoff by using Soil and Water Assessment Tool (SWAT), which is of critical importance for water resource
9 management, was investigated in this paper. Also, to specify the optimal DEM and LC resolutions for maximizing accuracy
10 of the estimated runoff for Dokan, Adhaim, and Duhok watersheds located in Iraq. Twenty daily time step based SWAT
11 models of each watershed were implemented using five DEMs in conjunction with five LCs. Assessment of models results
12 shows that the watershed delineation significantly affected by DEM resolution especially in flat regions. However, there is
13 no clearly discernible trend of this effect on the determination of watershed boundary, stream network, number of sub-basins
14 and total area. Furthermore, the number of Hydrologic Response Units (HRUs) and the maximum altitudes are directly
15 related to the DEM whereas the minimum altitudes have an inverse relationship with the DEM. Also, the number of HRUs
16 increases with the increase in LC resolution until it reaches a maximum value and then starts to gradually decrease. While
17 there is no significant trend between the accuracy of the estimated runoff and the increase in the DEM and LC resolutions.
18 The most accurate estimated runoffs of Dokan, Adhaim and Duhok Watersheds were obtained by using DEM 90 m and LC
19 1000 m, DEM 250 m and LC 1000 m, and DEM 30 m and LC 30 m with Nash and Sutcliffe Efficiency of 0.59, 0.68 and
20 0.69 respectively.

21 1 Introduction

22 Currently, hydrologic models employ satellite data such as Digital Elevation Model (DEM), Land Cover (LC), and soil data
23 as inputs to these models with a certain spatial resolution. Recently, Soil and Water Assessment Tool (SWAT) is considered
24 as one of the most useful tool for watershed modeling and management. It is important to understand the implications of
25 using currently available satellite data of different resolutions on hydrologic models behavior. The spatial input data of
26 hydrologic model raises several issues; A suitable spatial resolution of input data should be applied on the hydrologic model
27 to get accurate runoff simulation and watershed delineation, Does the high (finer) resolution of input spatial data gives better
28 runoff simulation than the low (coarser) resolution? and is the best resolution of input data used in specific watershed give
29 the same results for another different characteristics watershed in size and topography of watersheds?



30 Distributed hydrologic models divide the watershed into smaller units to represent heterogeneity within the watershed and
31 model outputs are affected by geomorphologic resolution (Arabi et al, 2006). More detail in the input data is required to
32 better describe spatial variability of the watershed. Proper model use requires an understanding of how model predictions
33 vary according to level of data aggregation and whether or not those variations can be attributed to differences in watershed
34 characteristics (FitzHugh and Mackay, 2001; Chang, 2009). Reducing the size and increasing the number of sub-units would
35 be expected to affect the simulation results from the entire watershed (Tripathi et al., 2006). Jayakrishnan et al. (2005),
36 concluded that application of SWAT is possible under lack of detailed digital data on land use, soil and elevation for model
37 input. Also, fine resolution input data and parameters calibration efforts, should improve the results. Reddy et al, (2015)
38 observed that reach lengths, reach slopes, sub-basins areas, and number of hydraulic Response Units (HRUs) varied
39 substantially due to DEM resolutions, also they found that the maximum altitude decreases, and the minimum altitude
40 increases, with decreasing DEM resolution. Tan et al, (2015), found that the total watershed area, number of sub-basins and
41 number of HRUs changed unevenly with DEM resolution. Also, Meins, (2013) found that there is no trend in the accuracy of
42 simulated flow when increasing the number of HRUs and defining the LC to matching default SWAT LC database leads to
43 more additional uncertainty. Chaplot, (2005) examined DEMs of 20 to 500 m spatial resolution. The results indicated that
44 the DEM resolution has a large influence on the simulated stream flow. Dixon et al, (2009) concluded that SWAT is indeed
45 sensitive to the resolution of the DEMs, original 90 and 30 m DEM resampled to 90 m did not show the same trend.
46 Therefore, the effects of resolution cannot be ignored and resampling may not be adequate in modeling stream flows using a
47 distributed watershed model. Lin et al, (2013) investigated DEMs such as Advanced Spaceborne Thermal Emission and
48 Reflection Radiometer (ASTER) 30 m and Shuttle Radar Topography Mission (SRTM) 90 m by SWAT model, the study
49 showed that accuracy of runoff simulation using SRTM 90 m is better than that of ASTER 30 m. Zhang et al, (2014)
50 assessed the sensitivity of SWAT model to the resolutions of DEMs. A range of 17 DEM spatial resolutions, from 30 to
51 1000 m, of Xiangxi River catchment area were considered. This assessment showed that the stream flow was essentially
52 unaffected by the DEM resolution. Romanowicz et al, (2005) evaluated the sensitivity of simulated runoff to the LC data in
53 Thyle catchment in Belgium by SWAT hydrologic model. The main conclusion of this evaluation was that the SWAT model
54 is extremely sensitive to the quality of the LC data. Arnold et al, (2005) investigated the accuracy of stream flow simulation
55 using two types of LC from different sources and resolutions, which are the LANDSAT-TM 30 m and AVHRR 1000 m
56 resolution by SWAT model. The result showed that the source of LC information did not affect the SWAT simulation of
57 stream flow. Mamillapalli et al. (1996) reported that there was a threshold beyond which higher resolution of data does not
58 produce better results of predicted runoff. Jha et al. (2004) and Chang (2009) recommend that watershed assessment based
59 on modeling should include a sensitivity analysis with varying sub-units size and number. There is not any established
60 method for determining the optimal sub watershed/hydrologic response unit (HRU) configuration.

61 In previous studies there is no agreement about impact of DEM and LC resolution on simulated runoff by SWAT model,
62 also a little attention had been given to the integrated impact of DEM and LC on simulated runoff and evaluating sensitivity
63 of SWAT model to characteristics of watershed such as size and variances on topography and LC. Therefore, three



64 watersheds of different characteristics were selected as the study area to assess the sensitivity of runoff modeling to DEM
65 and LC resolutions using SWAT model.

66 2 Materials and Methods

67 2.1 Runoff Simulation Model

68 SWAT is a semi-distributed physically based hydrological model developed by the United States Department of Agriculture
69 (USDA) (Arnold et al., 1998). The SWAT model can evaluate the impact of agricultural management on water, sediment
70 and agriculture chemical yield in ungauged basins (Arnold et al., 1998).

71 SWAT discretize the watershed into sub-basins based on DEM, the hydrologic parameters such as slope, area, and length of
72 sub-basins are extracted from the DEM, also, the DEM is used to extract channel properties such as channel length, width,
73 depth and slope (Rao et al., 2010). In SWAT, the sub-basins subdivided into HRUs that consist of homogeneous land use,
74 topographical, and soil characteristics (Arnold et al, 2011). The number and distribution of non-spatial HRUs created by
75 SWAT are related to the resolution of input spatial data when made the matching between slope, LC and soil, SWAT process
76 these HRUs to extract the hydrologic parameters and predict the evapotranspiration, surface runoff, groundwater flow and
77 sediment yield, etc. that take place at the HRU level. Furthermore, the water balance is simulated at this level before runoff
78 is routed to the reaches of the sub-basins and then to the basin channels (Neitsch et al. 2011). Accordingly, SWAT is
79 considered as the efficient tool to investigate the complementary interactive effects of DEM and LC resolution on runoff
80 simulation. Water balance equation, Eq. (1) is the fundamental base of SWAT:

81

$$82 \quad SW_t = SW_0 + \sum_{i=1}^t (R_{\text{day}} - Q_{\text{surf}} - ET_i - W_{\text{seep } i} - Q_{\text{gw}}) \quad (1)$$

83

84 Where SW_t is the final soil water content (mm), SW_0 is the initial soil water content on day i (mm), t is the time (days),
85 R_{day} is the precipitation on day i (mm), Q_{surf} is the surface runoff on day i (mm), ET_i is the evapotranspiration on day i (mm),
86 $W_{\text{seep } i}$ is the amount of water entering the vadose zone from the soil profile on day (Soil interflow) i (mm) and Q_{gw} is the
87 amount of return flow on day i (mm).

88 SWAT optionally provides the Soil Conservation Service Curve Number (SCS-CN) (USDA-SCS, 1972) method to estimate
89 the surface runoff and the Muskingum or variable storage method for flow routing in daily time base. Evapotranspiration can
90 be estimated using Hargreaves (Hargreaves et al., 1985), Priestley-Taylor (Priestley et al., 1972) or Penman-Monteith
91 (Monteith, 1965). Storage routing method is used to simulate the percolation process through soil layers. While the storage
92 model (Sloan et al., 1984) is used to estimate the lateral sub-surface flow.



93 2.2 Uncertainty and Sensitivity Analysis

94 Sensitivity analysis is performed using Latin Hypercube Sampling (LHS) and One At Time (OAT) methods (Hardyanto et
 95 al., 2007). To create multiple random samples, this method is started with LHS to divide the considered parameters range
 96 into intervals and then varying each of the LH points within these intervals. The number of changes must be equal to
 97 parameters number one at a time. Accordingly, the total effect is the average of the partial change in $S_{i,j}$ index of each
 98 parameter which is calculated using Eq. (2) (Van Griensven et al. 2006a), The highest sensitive parameter is given the first
 99 rank. While the rank of the lowest sensitive parameter can be equal to the total number of parameters.

100

$$101 \quad S_{i,j} = \left[\frac{100 \times \left(\frac{M(p_1, \dots, p_i + (1+f_i), \dots, p) - (p_1, \dots, p_i, \dots, p)}{M(p_1, \dots, p_i + (1+f_i), \dots, p) + M(p_1, \dots, p_i, \dots, p)} \right) / z}{f_i} \right] \quad (2)$$

102

103 Where M is the model function, f_i is the percentage change in parameter p for a LH point j .

104

105 The SWAT Calibration and Uncertainty Program (SWAT-CUP), is a software developed specially for calibration and
 106 uncertainty analysis of SWAT models. SWAT-CUP package software developed by Abbaspour (2011), includes five
 107 calibration programs (SUFI-2, PSO, GLUE, ParaSol and MCMC).

108 The Sequential Uncertainty Fitting version 2 (SUFI-2) is an algorithm of uncertainty parameters process the parameter
 109 ranges as the many tries steps to determine the most of the observed data within the 95 % band of estimation uncertainty.
 110 The overall uncertainty in output evaluated by the 95 % prediction uncertainty (95PPU). 95PPU calculated at the 2.5 % and
 111 97.5 % locations of the cumulative distribution of the simulated stream flow as output element. It extracted from Latin
 112 hypercube sampling (Abbaspour et al. 2007). The goodness of fit for calibration evaluated using the P-factor and the R-
 113 factor indicators. The P-factor is the percentage of observed data matched by the 95 PPU. It ranges from 0 to 1, where 1 is
 114 ideal value and means all of the observed data are within the model calculations. The R-factor is the mean width of the band
 115 divided by the standard deviation of the observed variable. It ranges from 0 to ∞ , where 0 indicates to perfect matching
 116 between simulated and observed. Based on the experience, an R-factor of around 1 is generally desirable (Abbaspour et al.,
 117 2007). SUFI-2 allows using different objective functions of optimization such as Nash–Sutcliffe efficiency (NS), Eq. (3),
 118 (Nash and Sutcliffe, 1970) or coefficient of determination R^2 , Eq. (5). NS and R^2 values greater than 0.5 are generally
 119 considered satisfactory and values greater than 0.75 are considered good (Gassman et al., 2007). Thus, the objective of the
 120 SUFI-2 is to maximize the P factor and to minimize the R factor, so that the optimal parameter range can be obtained. Global
 121 sensitivity analysis in SUFI-2 is calculated by plotting the Latin Hypercube generated parameters against the values of the
 122 objective function using multiple linear regression analysis. Then, a t-test is used to identify the relative significance for each
 123 parameter (Abbaspour et al. 2007). A more sensitive parameter has a greater t-test value and vice versa.

124



125
$$NS = 1 - \frac{\sum_i (Q_o - Q_s)_i^2}{\sum_i (Q_o - \bar{Q}_o)_i^2} \quad (3)$$

126

127
$$R^2 = \frac{[\sum_i (Q_{o,i} - \bar{Q}_o)(Q_{s,i} - \bar{Q}_s)]^2}{\sum_i (Q_{o,i} - \bar{Q}_o)^2 \sum_i (Q_{s,i} - \bar{Q}_s)^2} \quad (4)$$

128

129 Where, Q_o is the observed flow, Q_s is the simulated flow, \bar{Q}_o is the Average observed flow, and \bar{Q}_s is the average simulated
 130 flow.

131 2.2 Study Area

132 The study area was selected according to the data availability, watershed size and spatial variances of topographical and LC
 133 characteristics. Therefore, Dokan, Adhaim and Duhok watersheds which are the most important watersheds in Iraq were
 134 selected to be the study areas, Fig. 1. These watersheds are different in topography, size, and LC. Dokan and Adhaim
 135 watersheds have large areas with topographies of steep and flat slopes respectively. While Duhok Watershed has a small area
 136 with a topography of steep to mild slopes.

137 2.3.1 Dokan Watershed

138 Dokan Dam Watershed has an area of 11700 km². It is located between 36° 51' 16" to 35° 28' 26" N and 44° 26' 25" to 46°
 139 18' 16" E. Dokan basin covers an area within the north east of Iraq-Kurdistan region and north west of Iran. It is bounded by
 140 the Great Zab basin from the north whereas from the south it is adjoined by the Adhaim and Diyala Rivers basins. Dokan
 141 Dam was constructed on Lesser Zab Stream that origins in the Zagros Mountains in Iran at an elevation of 3000 m a.s.l.
 142 Herbs and shrubs covering predominantly the top of mountains and vegetation of the open oak forest (*Quercus* of *aegilops*)
 143 dominant the hilly regions. The river valleys are characterized by wet forested plants cover. While the foothill zone,
 144 especially the plain of Arbil, is heavily cultivated, patches of natural vegetation with herbs in the genus *Phlomis* being very
 145 common (Frenken et al., 2009).

146 2.3.2 Adhaim Watershed

147 Adhaim Dam Watershed is about 11600 km² located in northeast Iraq between 35° 42' 24" to 34° 33' 8" N and 43° 41' 9" to
 148 45° 27' 31" E. A network stream originates from mountain areas of elevation 1400-1800 m a.s.l. joining together at flat
 149 downstream area of an elevation of about 150 m a.s.l. creating Adhaim Stream. Barren land dominates the largest part of
 150 Adhaim Watershed, a few cultivated and orchards area of river irrigated in the western part of the watershed. The Cities of
 151 Kirkuk, Tuz Khormato, and other small towns located inside the watershed (Wahib et al., 2015).



152 **2.3.3 Duhok Watershed**

153 Duhok Dam Watershed is located on the far north of Iraq-Kurdistan region, between 37° 0' 25" to 36° 51' 53" N and 42° 50'
154 46" to 43° 5' 32" E. The total drainage area is 134.4 km². The watershed located in a mountainous area, mostly with very
155 deep and barren slopes due to soil erosion. The watershed consists of two main streams (Garmava and Linava) with small
156 river banks. The rocky slopes are total steep with more than 80 % decreasing in the direction along the stream, where they
157 are between 20 and 30 % in the northern part. Rangeland dominates the largest part of the watershed, a few forests and wood
158 land covering composed of dispersed oak trees and deciduous forest and shrubs on steep regions of the watershed, a small
159 part of the watershed is cultivated lands mainly located along the rivers. Rainy irrigated cultivated lands such as vineyards
160 can be found on the flat regions (Mohammed, 2010).

161 **2.4 Input Datasets**

162 The following datasets were collected, processed and used in this research:

163 **2.4.1 Digital Elevation Model (DEM)**

164 Nowadays, DEM become available as products of many satellites in different horizontal resolution and vertical accuracy. In
165 this research, five free cost global DEMs were used. These DEMs are:

- 166 i. Advanced spaceborne Thermal Emission and Reflection Radiometer (ASTER) DEM of 30 m spatial resolution (ASTER
167 GDEM Validation Team, 2009) with some improvements in absolute vertical accuracy of approximately 17 m and the
168 absolute horizontal accuracy is about ±30 m (Jarihani et al., 2015).
- 169 ii. Resampled DEM of 50 m spatial resolution. The majority resampling techniques (Tan et al, 2015) was used in
170 resampling ASTER DEM 30 to 50 m spatial resolution.
- 171 iii. Shuttle radar topography mission (SRTM) DEM of 90 m spatial resolution (SRTM, 2015).
- 172 iv. Resampled DEM of 250 m spatial resolution was produced from SRTM DEM of 90 m by using the majority resampling
173 techniques (Mou et al., 2015).
- 174 v. GTOPO30 DEM of 1000 m spatial resolution (GTOPO30, 2015).

175 The names, resolutions, and sources of these DEMs are listed in Table 1. The DEMs of Dokan, Adhaim and Duhok
176 Watersheds are shown in Figs. 2, 3 and 4 respectively. Since Duhok watershed is very small, only the DEM of 30, 50, 90 and
177 250 m spatial resolution was used in SWAT models of this watershed.

178 **2.4.2 Land Cover (LC)**

179 There are several institutions and research centers producing and publishing LC digital images with different spatial
180 resolutions. Some of these images are suitable for hydrological studies and available with free charge. In this research, five
181 types of LC images of spatial resolutions ranges between 15 to 1000 m were used. These images are:



- 182 i. Landsat LC of 15 m spatial resolution classified by Mohammed (2010).
- 183 ii. Landsat LC of 30 m spatial resolution. This image was classified by the National Geomatics Center of China (Chen,
184 2014).
- 185 iii. European Space Agency (ESA) LC of 300 m spatial resolution. This data was classified by ESA based on the United
186 Nations Land Cover Classification System (UN-LCCS) (Wei Li, 2016).
- 187 iv. Moderate Resolution Imaging Spectroradiometer (MODIS) LC of 500 m (Muchoney et al., 1999).
- 188 v. MODIS LC of 1000 m spatial resolution (Muchoney et al., 1999).

189 The names, resolutions, and sources of the used LC images are listed in Table 2. The LC images of Dokan, Adhaim and
190 Duhok Watersheds are shown in Figs. 5, 6 and 7 respectively. The LC image of 15 m spatial resolution was utilized only in
191 Duhok SWAT model because this watershed has a small area compared to other considered watersheds, whereas all other
192 LC images were utilized in SWAT models of Dokan, Adhaim and Duhok Watersheds.

193 **2.4.3 Soil Data**

194 Food and Agriculture Organization of the United Nations (FAO, 1995) supplies soil database of 5000 soil types. This data
195 comprising two layers (0 to 30 cm and 30 to 100 cm depth) at a spatial scale of 1:5000000. The data were downloaded from
196 (<http://www.fao.org/nr/land/soils/digital-soil-map-of-the-world/en>). The utilized soil maps in SWAT models for the Dokan,
197 Adhaim and Duhok watersheds are shown in Figs. 8, 9 and 10 respectively.

198 **2.4.4 Weather Data**

199 The Climate Forecast System Reanalysis (CFSR) dataset were used in this study (CFSR, 2015). CFSR provides the required
200 weather data such as precipitation, maximum and minimum temperatures, relative humidity, solar radiation, and wind speed
201 that used in SWAT for runoff simulation (Fuka et al, 2013 and Tomy et al, 2016). SWAT provides two options to input the
202 weather data, the simulated and gauged weather. In this research, the gauged mode was used. The data were downloaded
203 from (<http://globalweather.tamu.edu/>).

204 **2.4.5 Observed Runoff Data**

205 The recorded runoff of the periods from 2010 to 2013 for Dokan and Adhaim watersheds and from 2009 to 2013 for Duhok
206 watershed were used to calibrate and verify the SWAT models of these watersheds. The observed runoff data of Dokan and
207 Adhaim watersheds were provided by Iraqi Ministry of Water Resources (MoWR) which are unpublished documents, The
208 National Center for Water Resources Management/ Baghdad and Duhok Dam Directorate/Duhok Governorate provided the
209 observed runoff data for Duhok Watershed (unpublished documents).



210 **2.5 Model Setup**

211 In this research, ArcSWAT 2012 hydrologic model connected to ESRI ArcView 10.2.2 GIS software (ESRI 2014) was used
212 for runoff simulation, all of the spatial data were projected to the WGS1984-UTM Zone 38N projection. The threshold sub-
213 basin area of both Dokan, Adhaim and Duhok watersheds were setting on 200, 200 and 10 km² respectively. For all models
214 (Dokan, Adhaim and Duhok), slope is classified into five classes (0-10, 10-20, 20-30, 30-40 and >40) with multi slope
215 directions. The LC was reclassified by HRU definition window to matching SWAT default database of LC, this process was
216 completed depend on legends of classes that supplied by the LC producers, the data linked to the SWAT database by create
217 lookup tables in required format and connected with similar LC in default SWAT database. The soil map and database of
218 FAO were used for all models by adding the FAO soil database to SWAT user soil. The completed processing depends on
219 legends of soil classes that are attached with FAO soil maps, this data was linked to the SWAT user soil database by creating
220 lookup tables in required format and connected with added soil user database. Multiple HRUs created within each sub-basin,
221 and the threshold area setup on zero percent for slope, land cover, and soil data. In this step, all LC, soil, and slope classes in
222 a sub-basin were considered in creating the HRUs to represent all slopes, LC, soil classes without approximation.
223 The optional keys that were selected for the simulations of all models included: Runoff Curve Number (CN) method for
224 estimating surface runoff from precipitation, Penman-Monteith method for estimating potential evapotranspiration (ET), and
225 Variable Storage method to simulate stream water routing. All other SWAT default parameters were used as its original
226 values. The observed runoff data for the period from 1 Jan. 2010 to 31 Dec. 2013 were used to calibrate and validate Dokan
227 and Adhaim Watersheds models. Whereas that of the period from 1 Jan. 2009 to 31 Dec. 2013 were used to calibrate and
228 validate Duhok Watershed model.

229 **2.6 Calibration and Validation**

230 SWAT-CUP was used to perform the calibration and validation processes for all the considered models, by using the
231 Sequential Uncertainty Fitting version 2 (SUFI-2). In SUFI-2 the Nash–Sutcliffe efficiency (NS) set as objective function and
232 coefficient of determination (R^2) as minor indicator for evaluating the model performance. The data of the period from 1 Jan.
233 2010 to 31 Dec. 2011 were used for calibration and that of the period from 1 Jan. 2012 to 31 Dec. 2013 were used for
234 validation for both Dokan and Adhaim models. Whereas the data of the period from 1 Jan. 2009 to 31 Dec. 2011 were used
235 for calibration and that of the period from 1 Jan. 2012 to 31 Dec. 2013 were used for validation of Duhok models. The
236 suggested calibration parameters of Abbaspour et al, (2015a) and other parameters were used as trial to get most sensitive
237 parameters for each model. SWAT-CUP set up on 200 simulations in first iteration with (2 to 5) iterations for each model
238 (Abbaspour, 2015b). The second step, the models were run for validation period by using the best parameter ranges extracted
239 from calibration processing with the same number of simulations of last calibration iteration.



240 **3 Results and Discussions**

241 **3.1 Watersheds Boundaries and Stream Networks**

242 The DEM of a certain horizontal resolution has a particular vertical accuracy. Also, the DEM based method used in SWAT
243 is depended on altitudes of DEM to capture the desired point in determining the boundary or stream position of the
244 watershed. In flat topography regions, the variances on vertical altitudes are small this was reflected on the ability of DEM
245 based method to capture the desired altitudes and thus on watershed delineation.

246 The obtained delineations of Dokan, Adhaim and Duhok watersheds through applying the DEM based method in ArcSWAT
247 were as shown in Figs. 11 to 13. For Dokan watershed, the delineated boundary and stream network utilizing the 1000 m
248 DEM, Fig. 11, is significantly different from these delineated using other DEMs. While delineation of Adhaim watershed,
249 Fig. 12, shows that there is a large variation in the boundary and stream network that delineated using the considered five
250 DEMs. This large variation is very clear within the western side of this watershed because this side of the watershed has an
251 almost flat topography. In Duhok models, approximately all DEMs show same watershed boundary and stream network, Fig.
252 13. This is because the watershed surrounded by a steep mountain from all directions.

253 **3.2 Total Watersheds Area, Number of Sub-basins and Altitudes**

254 Different total areas of each watershed were computed as the DEM resolution of each watershed was changed, Table 3. The
255 total area of Duhok watershed, which is the smallest modeled watershed in this study, is gradually increased with the
256 decrease in DEM resolution. While no clear relationship was found between the total watershed area and DEM resolution for
257 the two large watersheds (Dokan and Adhaim). Also, it can be noticed that the number of sub-basins changed unevenly with
258 DEM resolution. The maximum number of sub-basins and the corresponding DEM resolution for Dokan, Adhaim and
259 Duhok watersheds were 35 (with 250 m DEM), 37 (with 50 m DEM) and 7 sub-basins (with 30, 50 and 90 m DEM)
260 respectively.

261 The estimated minimum and maximum ground elevation versus the DEM resolution for the considered watersheds is shown
262 in Fig. 14. This figure shows that there is an overestimate for the minimum elevations and underestimate for the maximum
263 elevations with the decrease (coarser) in DEM resolution. This is due to the loss of detailed topographic information at
264 coarser resolution.

265 **3.3 HRU Analysis**

266 Variation of HRUs number with LC for each DEM resolution was evaluated, Figure 15. This evaluation shows that with the
267 decrease (coarser) in DEM resolution the number of HRUs decreases for each LC resolutions. While the number of HRUs
268 increases with the decrease in LC resolution until a specific resolution and then recede. This because there are two
269 parameters controlling the number of HRUs for particular LC, which are the LC resolution and number of feature classes.
270 While for particular DEM one parameter controlled the number of HRUs, which is the slope.



271 3.4 Runoff Evaluation

272 The initial models of Dokan and Adhaim show up, high flow peaks, low base flow, and anteceded peaks (simulated shift to
273 left) in comparison with the observed flow. Unlike that for Duhok models, which show up high base flow, late peaks
274 (simulated shift to right) while the flow peaks were still high. Results of the best validated models are shown in Fig. 16. For
275 Dokan Watershed, the model of DEM 90 m resolution (SRTM) and LC of 1000 m resolution (MODIS) has the maximum
276 NS value than the other models with 0.59 and 0.61 of NS and R^2 respectively for the validation period. For Adhaim
277 Watershed, the model of DEM 250 m resolution (SRTM) and LC of 1000 m resolution (MODIS) achieved the best result
278 than the other models with 0.74 and 0.68 of NS and R^2 respectively for the validation period. While for Duhok Watershed
279 the model of DEM30 m resolution (ASTER) and LC of 30 m resolution (Landsat) achieved the best results with 0.69 and
280 0.69 of NS and R^2 respectively. These values are acceptable according to Abbaspour et al. (2007).

281 4 Conclusions

282 The sensitivity of SWAT hydrologic model to the resolution of input DEM and LC data for three watersheds of different
283 characteristics was examined. From the results, it can be concluded that variation of DEM resolution causes big variances in
284 watershed delineation, stream network position and total area. The watershed delineation, stream network position and total
285 area are highly effected by the DEM resolution and the characteristics of the watershed terrain especially in flat watersheds.
286 However, losses of detailed topographic information at coarser resolution produced an overestimate for the minimum
287 elevations and underestimate for the maximum elevations with the decrease (coarser) in DEM resolution. Also, the number
288 of sub-basins changed unevenly with the change in DEM resolution.

289 The results indicated that with the decrease in DEM resolution the number of HRUs decreases for each LC resolutions.
290 While the number of HRUs changed unevenly with LC resolution. In spite of, Adhaim Watershed is larger than Dokan
291 Watershed for all resulting models, the number of HRUs of Dokan is higher than that of Adhaim, because the variances of
292 slopes and LC in Dokan Watershed are higher than that of Adhaim Watershed. In other word, HRU is the matching between
293 the three elements of slope, LC, and soil creates the HRU, so the large variances in these three elements create large number
294 of HRU and vice versa.

295 Accordingly, the models of finer DEM and LC resolutions did not provide accurate runoff simulation by SWAT model, also
296 the large number of HRUs of higher data storage and longer time of run, calibration, and validation did not improve the
297 runoff simulation. This is because that the increase in the number of HRUs increases the hydrologic parameters and then
298 this leads to generate over parameterization. While the number of observed variables used in calibration is only the observed
299 flow and the uncertainty in LC data plays an important role when defining HRUs. The LC classes adjusted to matching the
300 default SWAT LC classes, this introduces much uncertainty on simulated runoff especially with the high number of HRUs.

301

302



303 **Acknowledgements**

304 Firstly, we would like to express our sincere gratitude to the faculty and technical staff of the Water and Hydraulic
305 Structures Engineering Branch in the University of Technology, Baghdad-Iraq for their valuable scientific assistance and
306 support. Also, we take this opportunity to express gratitude to Iraqi Ministry of Water Resources for providing the required
307 data and technical assistance.

308 It is inevitable that many people have contributed to this work, and we would like to acknowledge the support and assistance
309 we have received from several friends and colleagues.

310 **References**

311 Abbaspour K.C., Rouholahnejad E., Vaghefi S., Srinivasan R., Yang H., Kløve B.: A continental-scale hydrology and water
312 quality model for Europe: Calibration and uncertainty of a high-resolution large-scale SWAT model, *Journal of*
313 *Hydrology* 524 (2015) 733–752, 2015, a.

314 Abbaspour, K.C.: User Manual for SWAT-CUP, SWAT Calibration and Uncertainty Analysis Programs, Swiss Federal
315 Institute of Aquatic Science and Technology, Eawag, Duebendorf, Switzerland, page 25, 2015, b.

316 Arabi, M., R.S. Govindaraju, M.M. Hantush, and B.A. Engel: Role of watershed subdivision on modeling the effectiveness
317 of best management practices with SWAT, *Journal of the American Water Resources Association* 42(2): 513-528,
318 2006.

319 Arnold, J.G., Srinivasan, R., Muttiah, R.S., Williams, J.R.: Large area hydrologic modeling and assessment e part 1: model
320 development, *J. Am. Water Resour. Assoc.* 34, 73e89, 1998.

321 Arnold J. G., Moriasi D. N., Gassman P. W., Abbaspour K. C., White M. J., Srinivasan R., Santhi C., Harmel R. D., van
322 Griensven A., Van Liew M. W., Kannan N., Jha M. K.: SWAT model use, calibration and validation, Vol. 55(4):
323 1491-1508 *Transactions of the ASABE*, American Society of Agricultural and Biological Engineers ISSN 2151-0032,
324 2011.

325 Arnold Jeff G., Chen Pei-yu, Mauro Di Luzio: Impact of two land cover sets on stream flow and total nitrogen simulations
326 using a spatially distributed hydrologic mode. Pecora 16 “Global Priorities in Land Remote Sensing” October 23-27,
327 2005, Sioux Falls, South Dakota, 2005.

328 ASTER GDEM Validation Team: ASTER Global DEM Validation Summary Report,
329 http://www.ersdac.or.jp/GDEM/E/image/ASTERGDEM_ValidationSummaryReport_Ver1.pdf (accessed 15.07.15),
330 2009.

331 Chang, C. L.: The impact of watershed delineation on hydrology and water quality simulation, *Environ Monit Assess*
332 148(1):159–165, 2009.

333 Chaplot V.: Impact of DEM mesh size and soil map scale on SWAT runoff, sediment, and NO₃-N loads predictions, *Journal*
334 *of Hydrology* 312 (2005) 207–222, 2005.



- 335 Chen L.: 30-meter global land cover dataset (globalland30), <http://www.globallandcover.com/GLC30Download/index.aspx>,
336 2014.
- 337 Climate Forecast System Reanalysis (CFSR) dataset: <http://globalweather.tamu.edu/>, 2015.
- 338 Dixon B.: Resample or not?! Effects of resolution of DEMs in watershed modeling. *Hydrological Processes*, 23, 1714–1724,
339 2009.
- 340 FitzHugh, T.W. and D.S. Mackay: Impact of sub watershed partitioning on modeled source and transport – limited sediment
341 yields in an agricultural nonpoint source pollution model, *J. Soil and Water Conservation* 56(2): 137-143, 2001.
- 342 Food and Agricultural Organization (FAO): The Digital Soil Map of the World and Derived Soil Properties [CD-ROM],
343 Version 3.5, Rome, 1995.
- 344 Frenken, Karen: Irrigation in the Middle East Region in Figures. AQUASTAT Survey 2008, Water Reports, 34, Rome:
345 FAO, ISBN 978-92-5-106316-3, 2009.
- 346 Fuka D. R., Walter T. M., MacAlister C., Degaetano A. T., Steenhuis T. S., Easton Z. M.: Using the climate forecast system
347 reanalysis as weather data for watershed modelling, *Hydrological Processes* DOI:10.1002/hyp.10063, 2013.
- 348 GTOPO30: Global digital elevation model. <http://earthexplorer.usgs.gov/>, 2015.
- 349 Jayakrishnan, R., R. Srinivasan, C. Santhi and J. G. Arnold: Advances in the application of the SWAT model for water
350 resources management, *Hydrol. Process.* 19: 749–762, 2005.
- 351 Jha, M., P.W. Gassman, S. Secchi, R. Gu, and J. Arnold: Effect of watershed subdivision on SWAT flow, sediment, and
352 nutrient predictions, *JAWRA* 40(3): 811-825, 2004.
- 353 Lin, S., Jing, C. W., Coles, N., Chaplot, V., Moore, N., & Wu, J. P.: Evaluating DEM source and resolution uncertainties in
354 the soil and water assessment Tool. *Stochastic Environmental Research and Risk Assessment*, 27(1), 209e221, 2013.
- 355 Mamillapalli, S., R. Srinivasan, J. G. Arnold, B. A. Engel: Effect of spatial variability on basin scale modelling, *Proceedings*
356 *of the 3rd International Conference on Integrating GIS and Environmental Modeling*, January 21-26, Santa Fe, NM.,
357 USA, 1996.
- 358 Meins F. M.: Evaluation of spatial scale alternatives for hydrological modelling of the Lake Naivasha basin, Kenya, Master
359 thesis, University of Twente, 2013.
- 360 Mohammed R. H.: The Impact Of The Man Activity in Duhok Dam Watershed On The Future Of Duhok Dam Lake North-
361 Iraq, The 1 st International Applied Geological Congress, Department of Geology, Islamic Azad University - Mashad
362 Branch, Iran, 26-28 April 2010.
- 363 Mou Leong Tan, Darren L. Ficklin, Barnali Dixon, Ab Latif Ibrahim, Zulkifli Yusop, Vincent Chaplot: Impacts of DEM
364 resolution, source, and resampling technique on SWAT-simulated stream flow, *Applied Geography* 63 (2015) 357e368,
365 2015.
- 366 Muchoney, D., Strahler, A., Hodges, J., & Lo Castro, J.: The IGBP DIS Cover Confidence Site and the System for Terrestrial
367 Ecosystem Parameterization: Tools for Validating Global Land Cover Data, *Photogrammetric Engineering and*
368 *Remote Sensing*, 65(9), 1061---1067, .1999.



- 369 Neitsch, S. L., Arnold, J. G., Kiniry, J. R., & Grassland, J. R. W.: Soil and water assessment tool theoretical documentation
370 version 2009, Texas Water resources Institute Technical Report No. 406. Texas: Texas A&M University, 2011.
- 371 Rao, M. N., Yang, Z.: Groundwater impacts due to conservation reserve program in Texas County, Oklahoma. *Applied*
372 *Geography*, 30(3), 317e328, 2010.
- 373 Reddy S., Reddy M J.: Evaluating the influence of spatial resolutions of DEM on watershed runoff and sediment yield using
374 SWAT, *Earth Syst. Sci.* 124, No. 7, October 2015, pp. 1517–1529, 2015.
- 375 Romanowicz A.A., Vancloster M., Rounsevell M., Junesse I. La: Sensitivity of the SWAT model to the soil and land use
376 data parametrisation: a case study in the Thyle catchment, Belgium. *Ecological Modelling* 187 (2005) 27–39, 2005.
- 377 SRTM: Global digital elevation model. [http://glcf.umd.edu /data/srtm/](http://glcf.umd.edu/data/srtm/), 2015.
- 378 Tomy T., Sumam K. S.: Determining the Adequacy of CFSR Data for Rainfall-Runoff Modeling Using SWAT, *Procedia*
379 *Technology* 24 (2016) 309 – 316, 2016.
- 380 Tripathi, M.P., N.S. Raghuwanshi and G.P. Rao.: Effect of watershed subdivision on simulation of water balance
381 components, *Hydrol. Process.* 20(3): 1137-1156, 2006.
- 382 Wahib N. R., Al amau: Climate controls and determinants of Diyala province,. *Diyala Journal Issue* 67, 2015.
- 383 Wei Li, Ciais P., MacBean N , Peng S., Defourny P. & Bontemps S.: Major forest changes and land cover transitions based
384 on plantfunctional types derived from the ESA CCI Land Cover product, *International Journal of Applied Earth*
385 *Observation and Geo information* 47 , 30–39, 2016.
- 386 Wolock, D. M., Price, C. V.: Effects of digital elevation model map scale and data resolution on a topography-based
387 watershed model, *Water Resources Research*, 30(11), 3041e3052, 1994.
- 388 Zhang Peipei, Liu Ruimin, Yimeng Bao, Wang, Jiawei Wenwen Yu, Zhenyao Shen: Uncertainty of SWAT model at
389 different DEM resolutions in a large mountainous watershed, *Water research* 53. 132 e144, 2014.

390

391

392

393

394

395

396

397

398

399

400

401

**Table 1.** Utilized DEMs in SWAT models of Dokan, Adhaim and Duhok Watersheds Watershed.

No	Name	Spatial resolution	Source
1	ASTER GDEM2	30 m	http://gdex.cr.usgs.gov/gdex/
2	Resampled from ASTER	50 m	http://gdex.cr.usgs.gov/gdex/
3	SRTM v4.1	90 m	http://srtm.csi.cgiar.org/
4	SRTM	250 m	http://srtm.csi.cgiar.org/
5	GTOPO	1000 m	http://earthexplorer.usgs.gov/

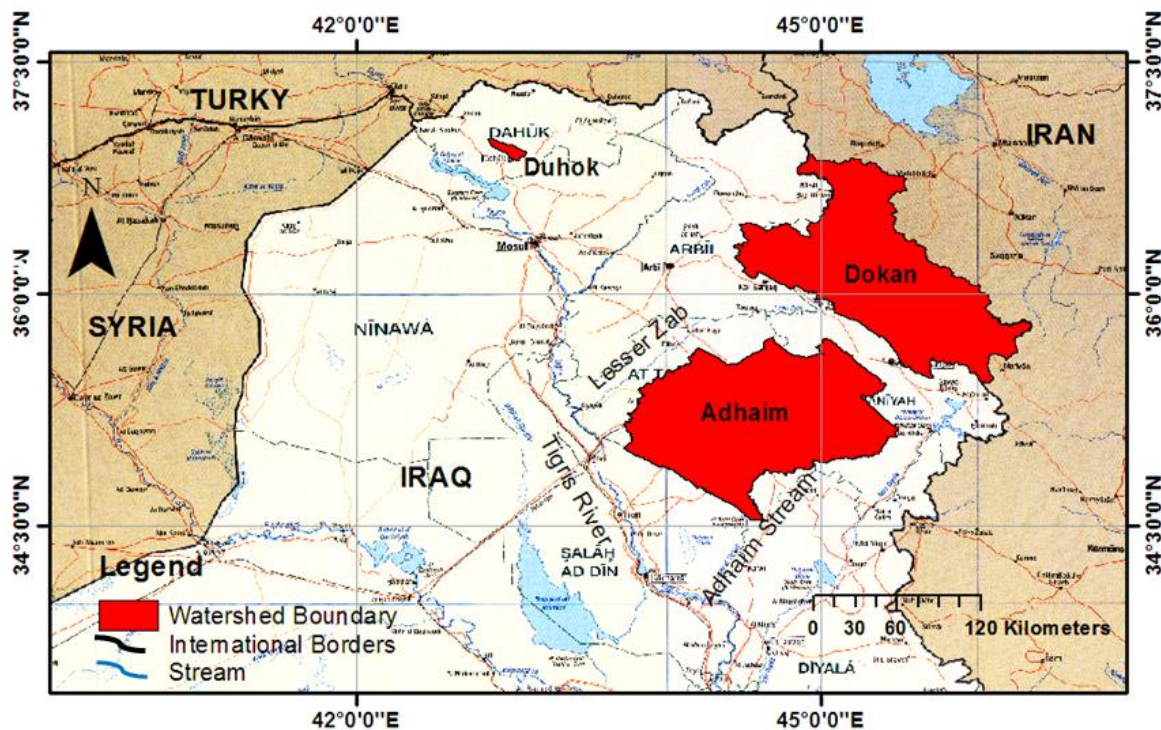
Table 2. Utilized LC data in SWAT models of Dokan, Adhaim and Duhok Watersheds.

No	Name	Spatial	Source
1	Landsat	15 m	Mohammed, 2010
2	Landsat	30 m	http://www.globallandcover.com/
3	ESA	300 m	http://maps.elie.ucl.ac.be/CCI/viewer/download.php
4	MODIS	500 m	http://gdex.cr.usgs.gov/gdex/
5	MODIS	1000m	http://gdex.cr.usgs.gov/gdex/

Table 3. Total area of Dokan, Adhaim and Duhok Watershed.

DEM resolution	Dokan		Adhaim		Duhok	
	Total area (km ²)	No. of sub-basins	Total area (km ²)	No. of sub-basins	Total area (km ²)	No. of sub-basins
30	11499	33	12013	33	133.8	7
50	11357	33	12116	37	134.5	7
90	11336	33	11910	35	135	7
250	11558	35	11901	31	137.5	5
1000	11552	31	11979	33	*	*

*indicated no model in this resolution.

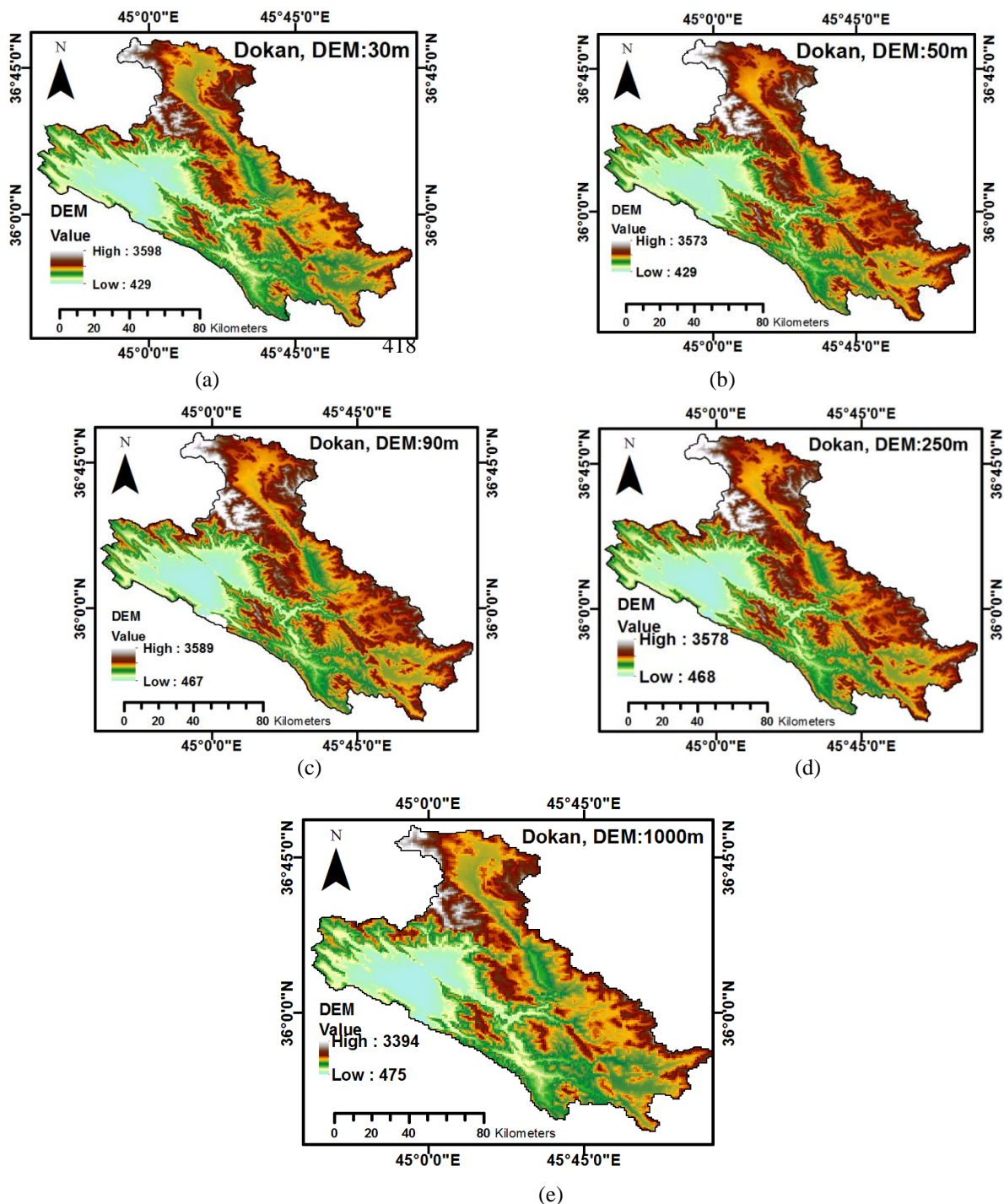


414
415
416

Figure 1. Location of study area.



417



419

420

421

422

423

424

425

426

427

428

429

430

431

432

433

434

435

436

437

438

439

440

441

442

Figure 2. The DEMs utilized in SWAT models for Dokan Watershed; (a) Dokan DEM 30 m, (b) Dokan DEM 50 m, (c) Dokan DEM 90 m, (d) Dokan DEM 250 m, (e) Dokan DEM 1000 m.

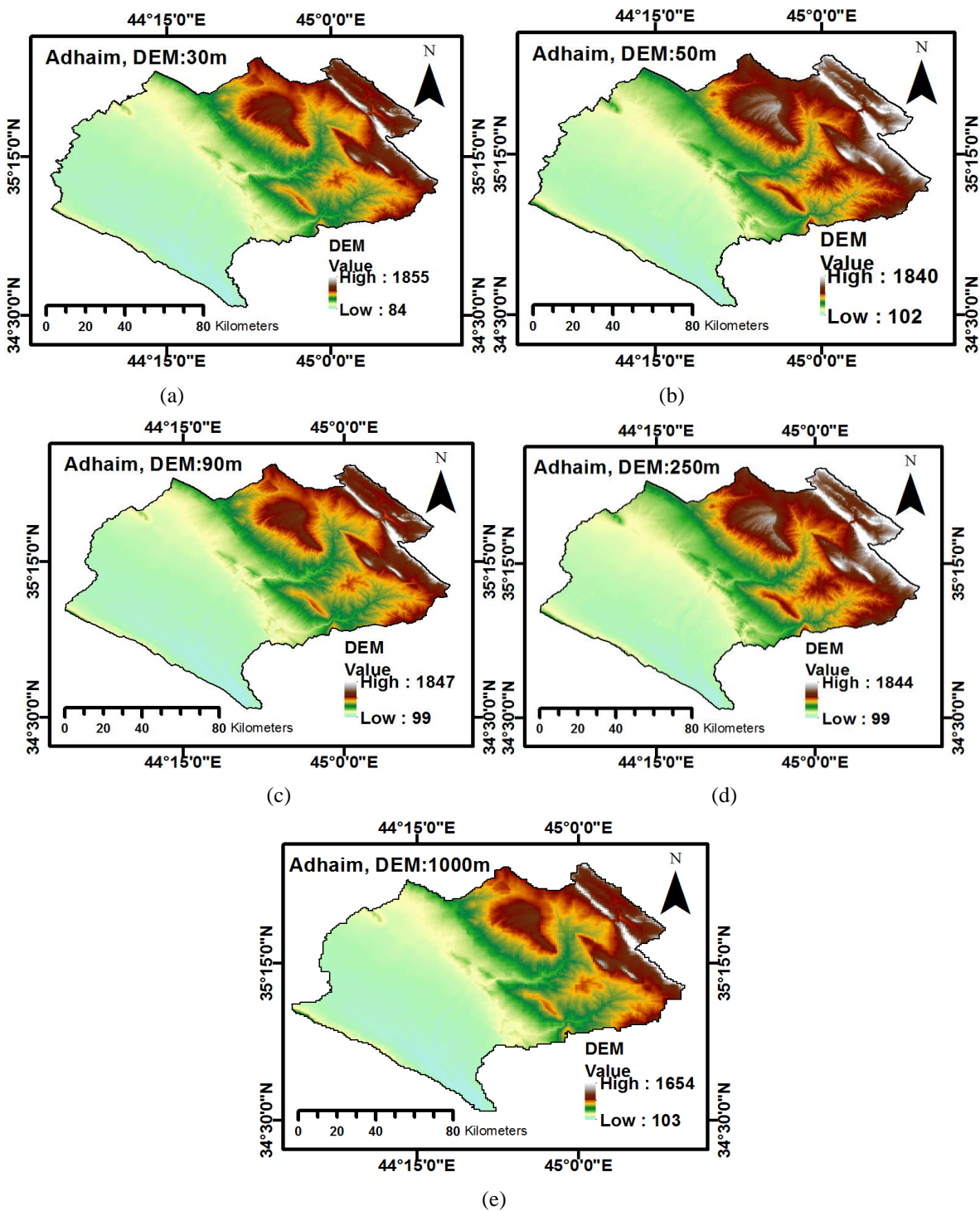
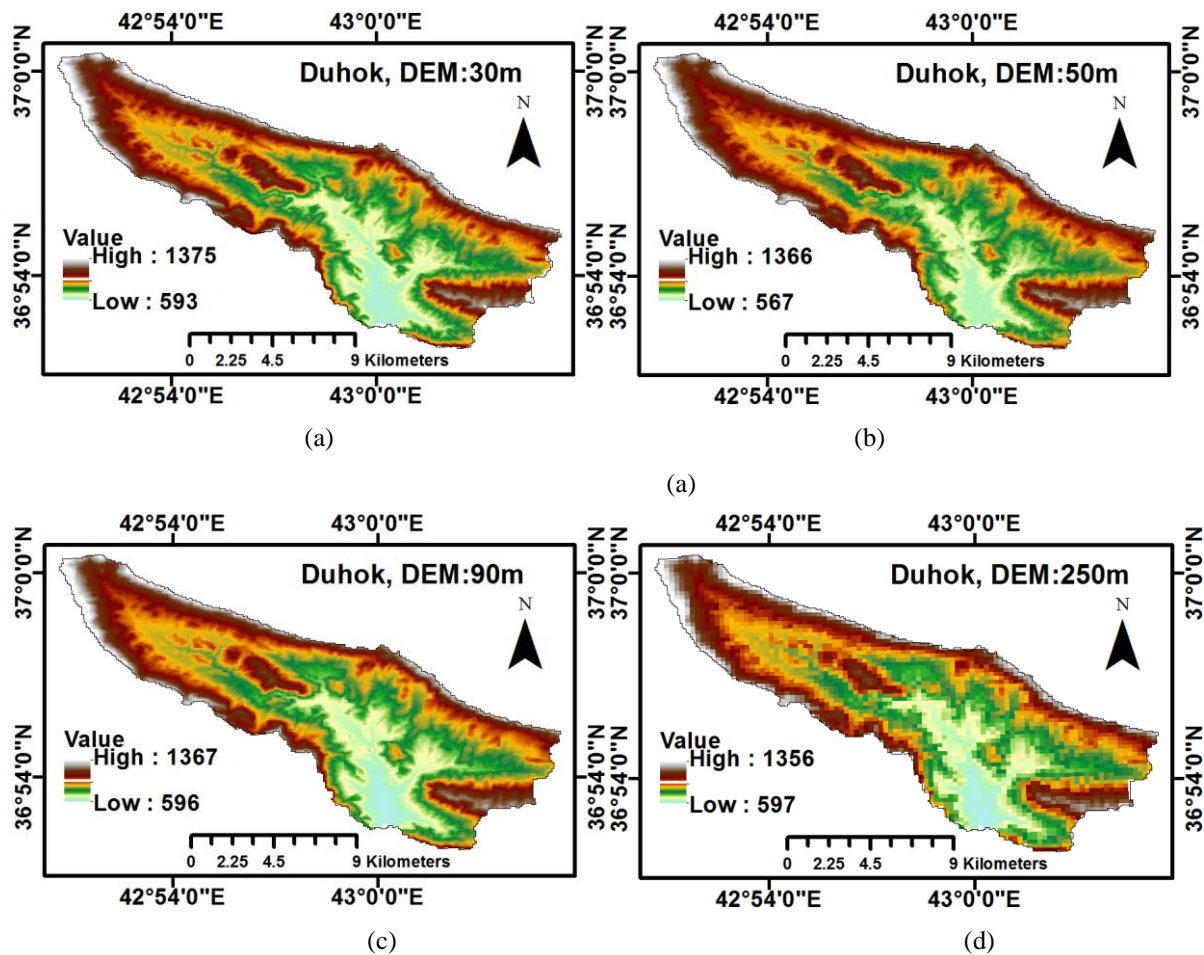


Figure 3. The DEMs utilized in SWAT models for Adhaim Watershed; (a) Adhaim DEM 30 m, (b) Adhaim DEM 50 m, (c) Adhaim DEM 90 m, (d) Adhaim DEM 250 m, (e) Adhaim DEM 1000 m.



451



452

453

454

455

456

457

458

459

460

461

462

463

464

465

466

467

468

Figure 4. The DEMs utilized in SWAT models for Duhok Watershed; (a) Duhok DEM 30 m, (b) Duhok DEM 50 m, (c) Duhok DEM 90 m, (d) Duhok DEM 250 m.

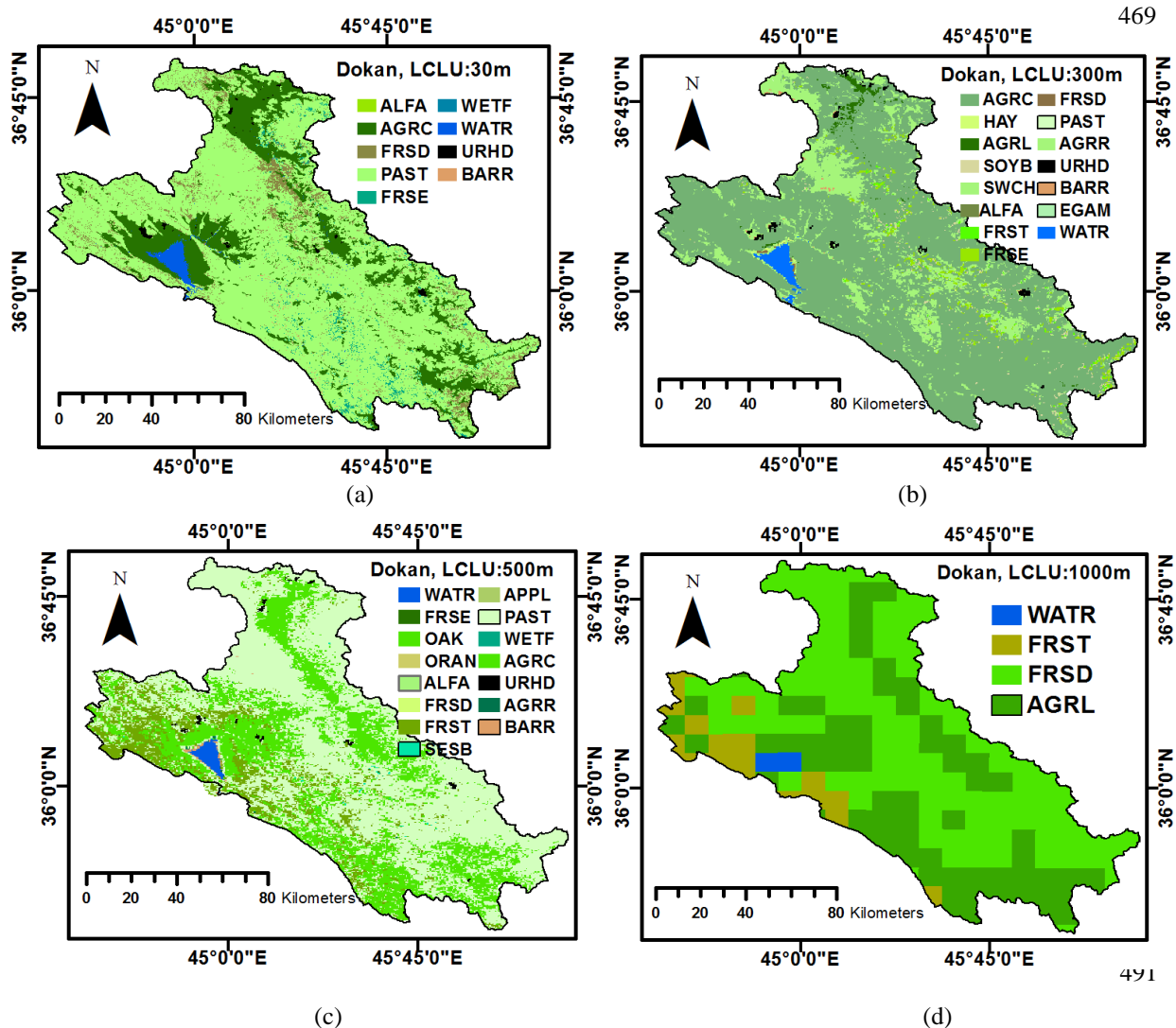


Figure 5. The LC utilized in SWAT models for Dokan Watershed; (a) Dokan LC 30 m, (b) Dokan LC 300 m, (c) Dokan LC 500 m, (d) Dokan LC 1000 m.

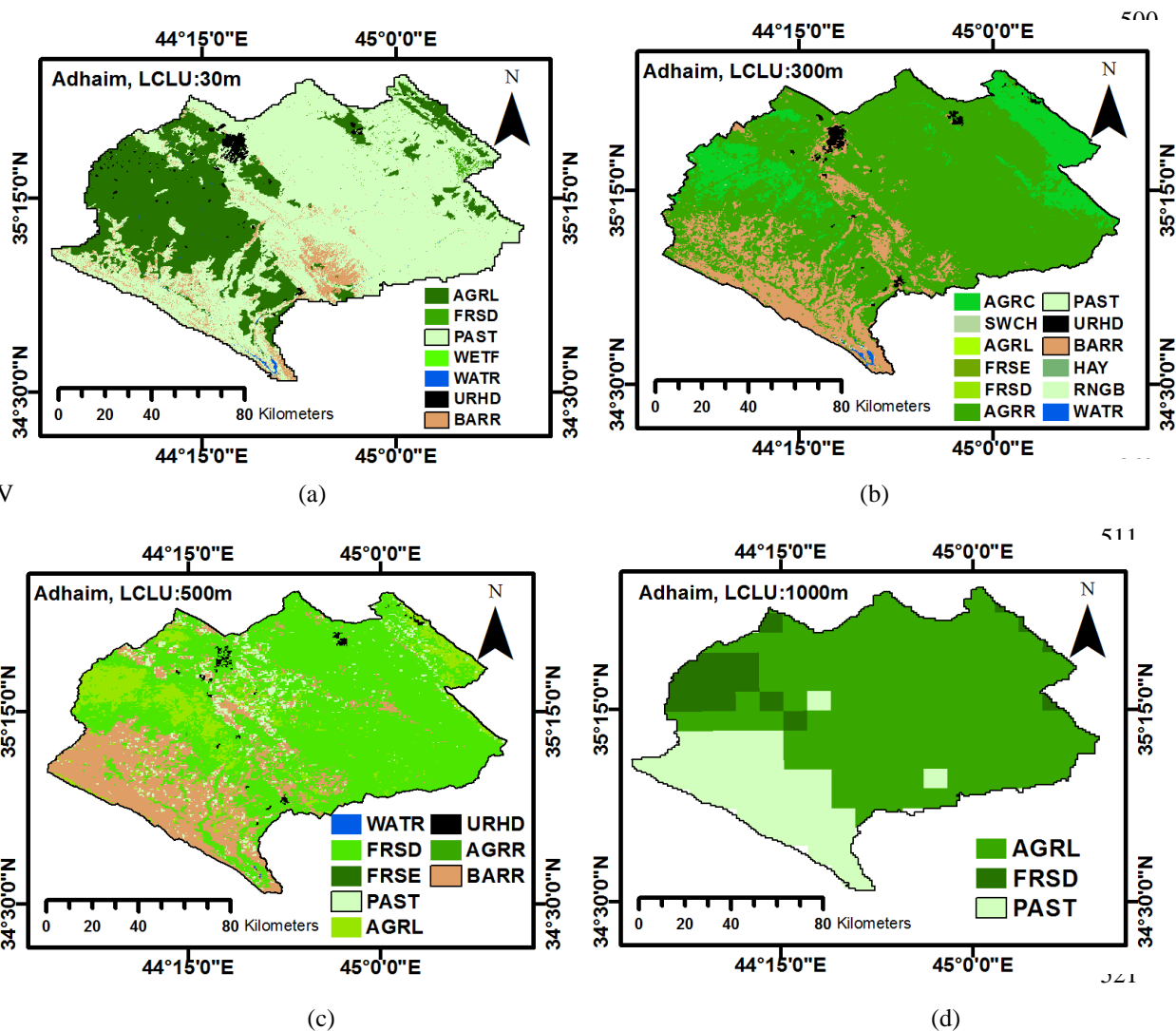
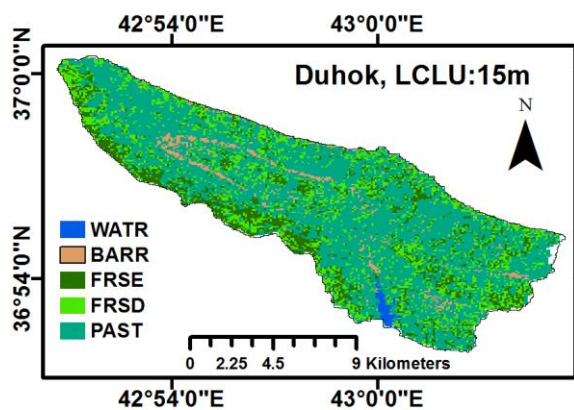
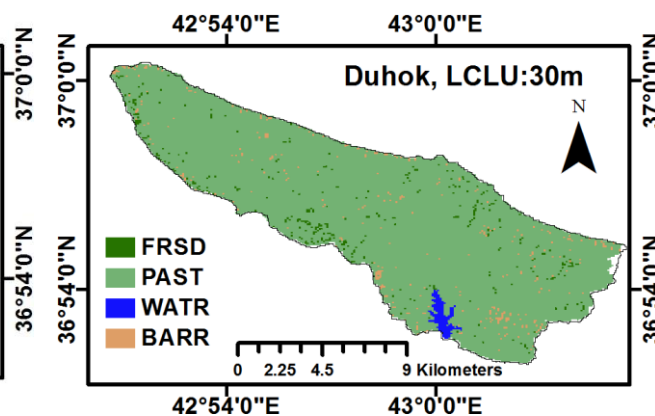


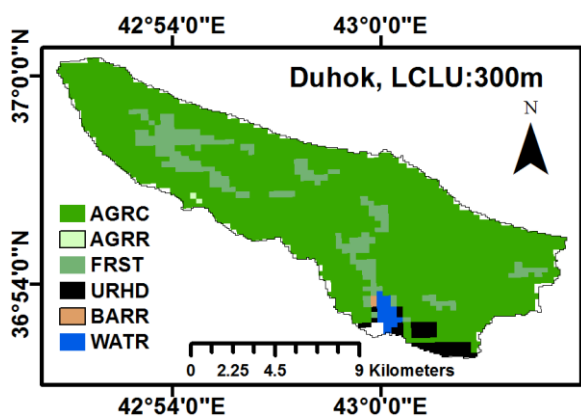
Figure 6. The LC utilized in SWAT models for Adhaim Watershed: (a) Dokan LC 30 m, (b) Dokan LC 300 m, (c) Dokan LC 500 m, (d) Dokan LC 1000 m.



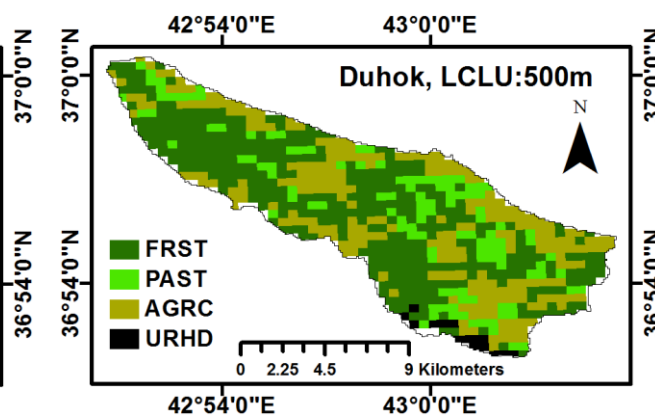
(a)



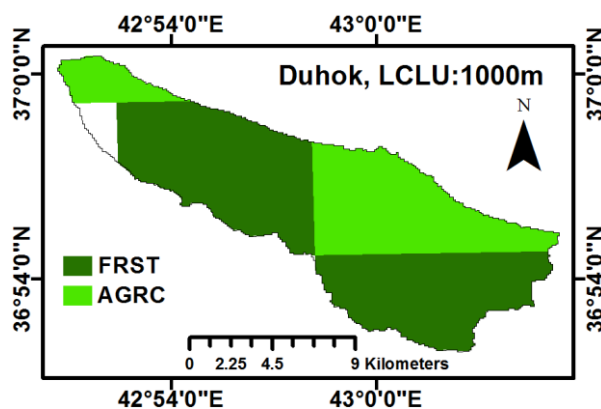
(b)



(c)



(d)



(e)

562 **Figure 7.** The LC utilized in SWAT models for Duhok Watershed; (a) Duhok LC 15 m, (b) Duhok LC 30 m, (c) Duhok LC
 563 300 m, (d) Duhok LC 500 m, (e) Duhok LC 1000 m.

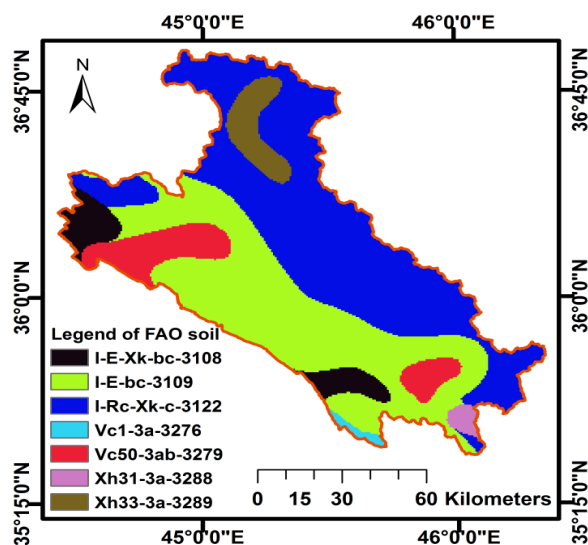


Figure 8. Utilized soil map in SWAT model of Dokan watershed.

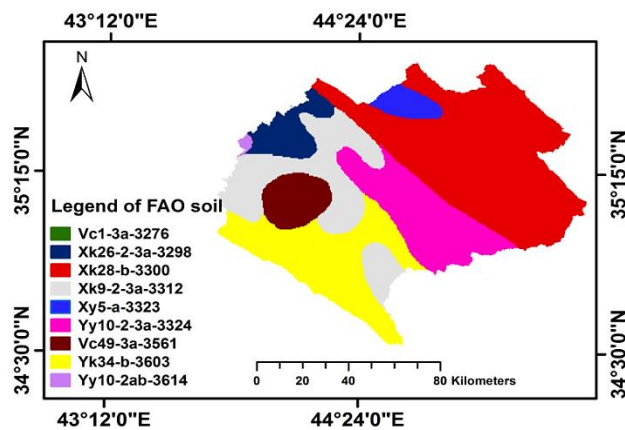


Figure 9. Utilized soil map in SWAT model of Adhaim watershed.

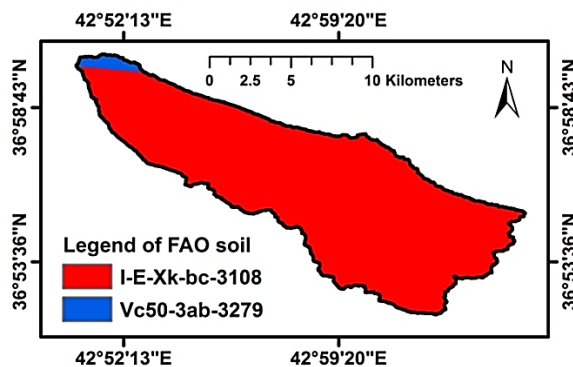
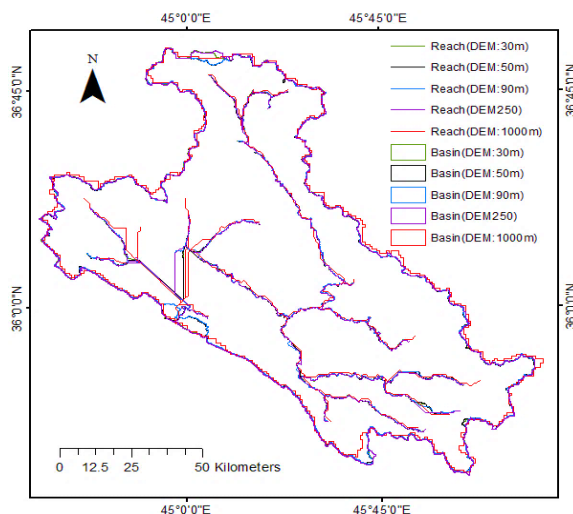


Figure 10. Utilized soil map in SWAT model of Duhok watershed.

564
565
566

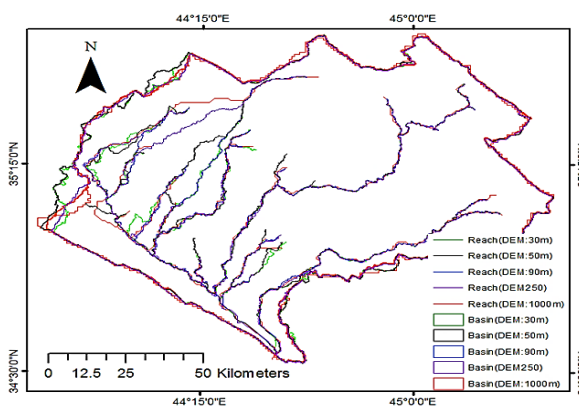
567
568

569
570



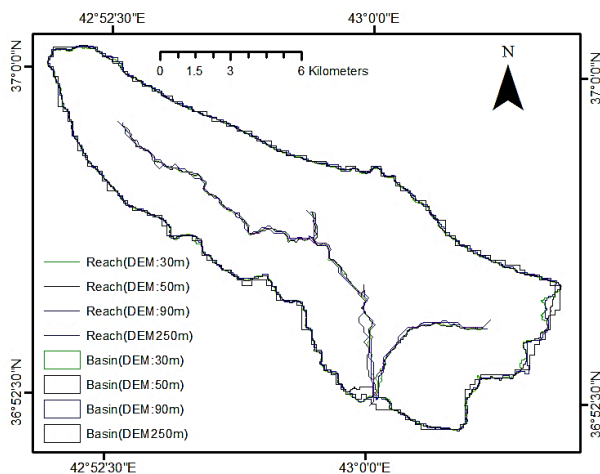
571
572

Figure 11. Delineation of Dokan watershed.



573
574

Figure 12. Delineation of Adhaim watershed.



575
576

Figure 13. Delineation of Duhok watershed.

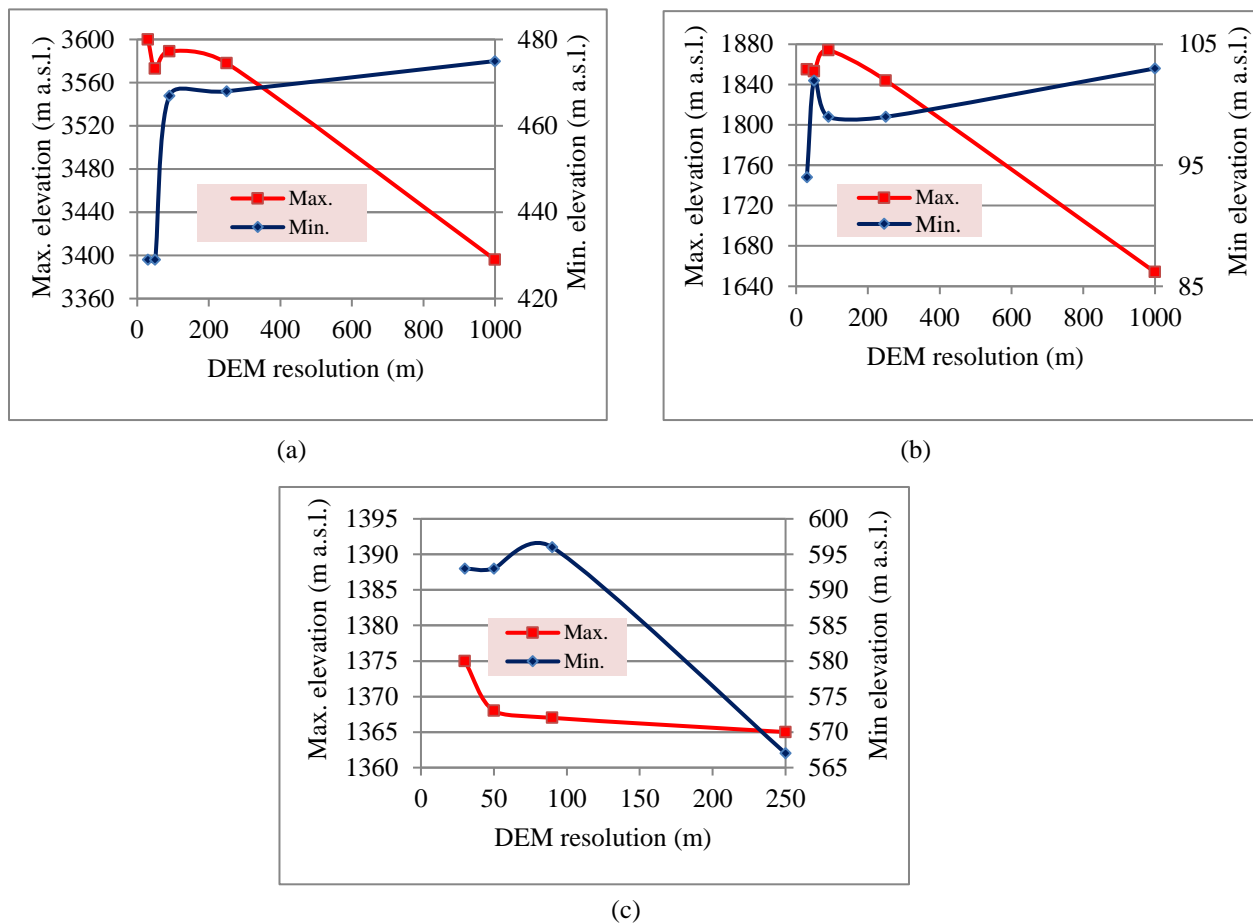
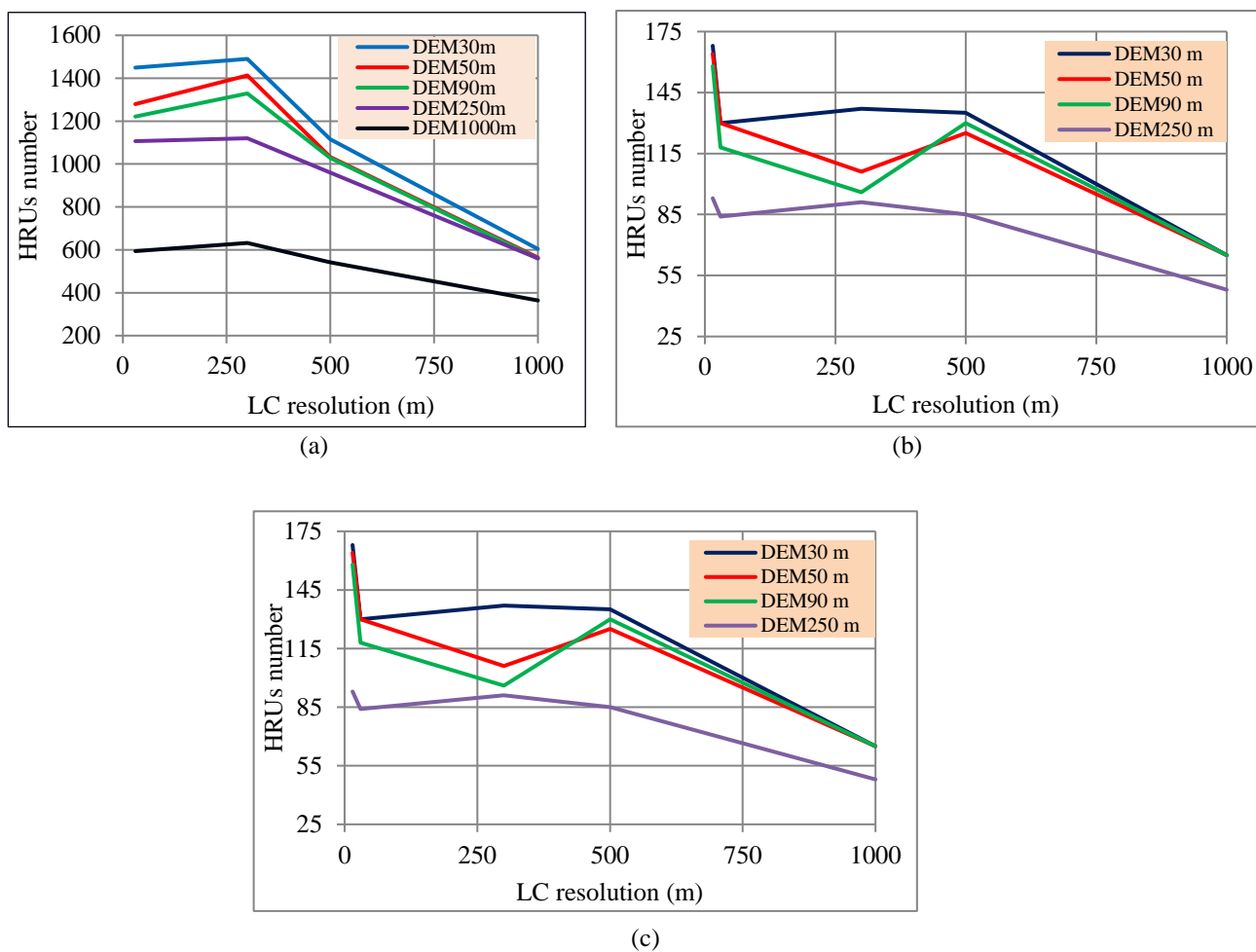


Figure 14. Minimum and Maximum ground elevation for different DEM resolution; (a) Dokan watershed, (b) Adhaim watershed, (c) Duhok watershed.



606



607

608

609

610

611

612

613

614

615

616

617

618

619

620

621

622

623

624

625

626

627

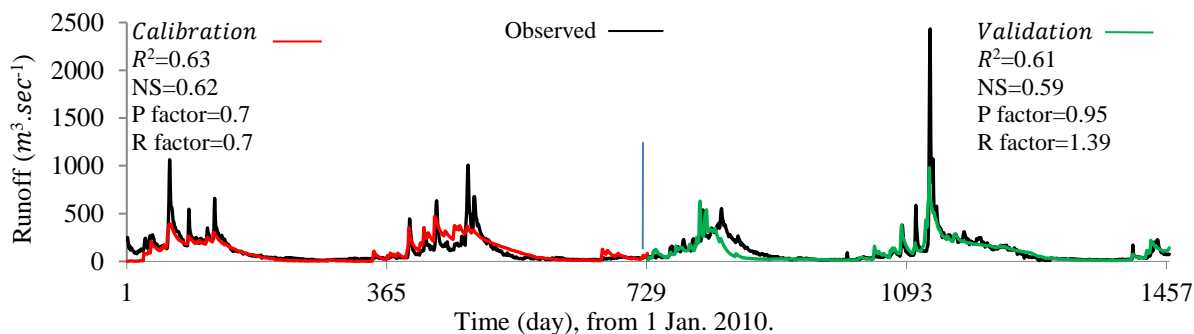
628

629

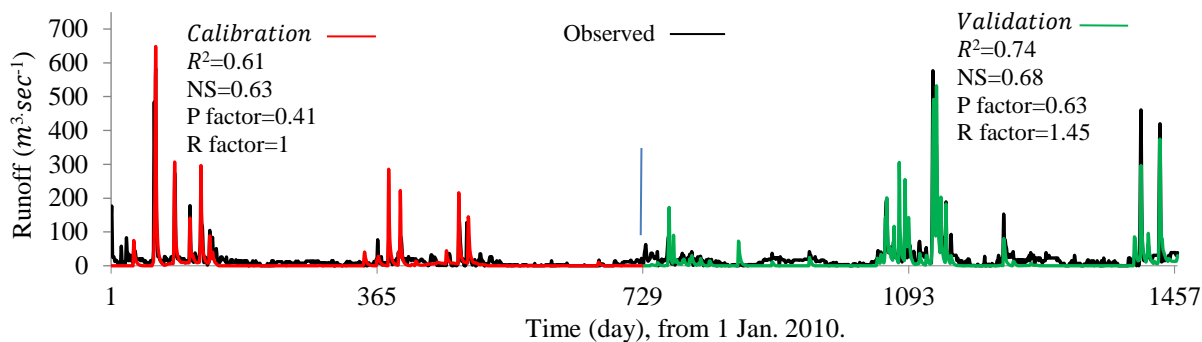
Figure 15. HRUs number of the watersheds versus DEM and LC resolution; (a) Dokan watershed, (b) Adhaim watershed, (c) Duhok watershed.



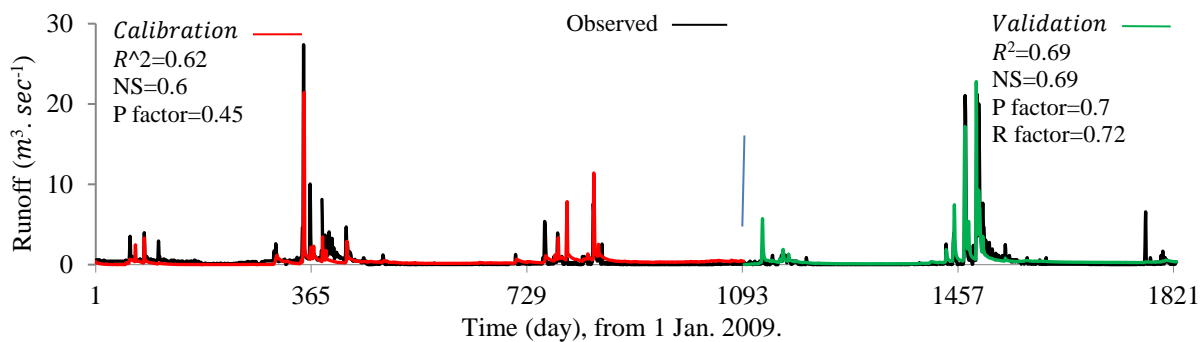
630
 631



632
 633
 634
 635



636
 637
 638



639
 640
 641
 642

Figure 16. Results of the best validated models; (a) Dokan model (DEM250m, LC1000m),
 (b) Adhaim model (DEM250m, LC1000m), (c) Duhok model (DEM30m, LC30m).